

UNCLASSIFIED

AD NUMBER

AD261942

LIMITATION CHANGES

TO:

Approved for public release; distribution is unlimited.

FROM:

Distribution authorized to U.S. Gov't. agencies and their contractors;  
Administrative/Operational Use; AUG 1961. Other requests shall be referred to Air Force Systems Command, Arnold Engineering Development Center, Tullahoma, TN 37389.

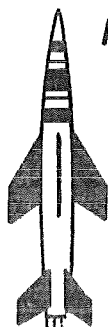
AUTHORITY

aedc per dtic form 55

THIS PAGE IS UNCLASSIFIED

AEDC-TN-61-90

ARCHIVE COPY  
DO NOT LOAN



**AERODYNAMIC PERFORMANCE OF A THIRD STAGE  
PLENUM EVACUATION COMPRESSOR OF THE  
ARNOLD CENTER PROPULSION WIND TUNNEL**

By

B. B. Estabrooks, R. A. Robinson, and M. H. Jones  
PWT, ARO, Inc.

August 1961

**ARNOLD ENGINEERING  
DEVELOPMENT CENTER**

**AIR FORCE SYSTEMS COMMAND**

AEDC TECHNICAL LIBRARY



*Additional copies* of this report may be obtained from

ASTIA (TISVV)  
ARLINGTON HALL STATION  
ARLINGTON 12, VIRGINIA

**note**

Department of Defense contractors must be established for ASTIA services, or have their need-to-know certified by the cognizant military agency of their project or contract.

AERODYNAMIC PERFORMANCE OF A THIRD STAGE  
PLENUM EVACUATION COMPRESSOR OF THE  
ARNOLD CENTER PROPULSION WIND TUNNEL

By

B. B. Estabrooks, R. A. Robinson, and M. H. Jones  
PWT, ARO, Inc.

July 1961

ARO Project No. 245903  
Contract No. AF40(600)-800 S/A 24(61-73)



## ABSTRACT

The aerodynamic performance of a third stage compressor of the Plenum Evacuation System of the Propulsion Wind Tunnel Facility was determined at inlet guide vane angle settings for minimum, design, and maximum capacities. In addition to the normal steady-state pressure and flow measurements, transient measurements of the pressures in the ducts adjacent to the compressor were obtained during definition of the compressor stall boundary.

The compressor realized a maximum stall boundary pressure ratio of 2.15 to 2.26 with variation of inlet guide vane angle from +15 to -15 deg at an inlet temperature of 100°F. At the compressor design pressure ratio of 2.00 the measured inlet volume flow was 1285 and 1485 cfs at minimum (+15 deg) and maximum (-15 deg) inlet guide vane angle settings, respectively. The measured compressor adiabatic efficiency at the design condition was 87 percent.

Measurements were also obtained that defined a double-valued compressor characteristic, composed of the normal characteristic and a stalled branch of the characteristic. The compressor operation along the stalled branch of the characteristic after stall inception was dependent upon the bypass throttling characteristic.



## CONTENTS

	<u>Page</u>
ABSTRACT . . . . .	3
NOMENCLATURE . . . . .	7
INTRODUCTION . . . . .	9
APPARATUS	
Facility . . . . .	9
Plenum Evacuation System . . . . .	10
Instrumentation . . . . .	10
TEST PROCEDURE . . . . .	11
DATA REDUCTION PROCEDURE . . . . .	12
RESULTS AND DISCUSSION	
Steady-State Compressor Characteristics . . . . .	13
Compressor Double-Valued Performance Characteristic . . . . .	14
Transient Compressor Measurements . . . . .	16
CONCLUDING REMARKS . . . . .	19
REFERENCES . . . . .	20

## ILLUSTRATIONS

<u>Figure</u>	
1. The PWT Facility Layout . . . . .	21
2. View of the Plenum Evacuation System (Second Increment). . . . .	22
3. Third Stage Compressor and Associated Ducts . . . . .	23
4. Schematic of Plenum Evacuation System . . . . .	24
5. Layout of Third Stage Compressor Ducts and Aerodynamic Instrumentation Locations . . . . .	25
6. Dimensions and Details of Rake Installations . . . . .	26
7. Layout of Third Stage Compressor Bypass Ducts Arrangement . . . . .	27
8. Measured Compressor Performance at 100°F Inlet Temperature . . . . .	28
9. Comparison of Total and Static Compressor Pressure Ratios . . . . .	29
10. Measured Compressor Performance at 135°F Inlet Temperature . . . . .	30



<u>Figure</u>		<u>Page</u>
11.	Comparison of Measured and Predicted Compressor Performance . . . . .	31
12.	Maximum Inlet Pressure versus Static Pressure Ratio of the Third Stage as Limited by Coupling Rating of 3800 hp . . . . .	32
13.	Compressor Double-Valued Characteristics . .	33
14.	Transient Compressor Measurements - Compressor Stall . . . . .	34
15.	Transient Compressor Measurements - Compressor Surge and Stall . . . . .	35
16.	Transient Compressor Measurements - Compressor Surge . . . . .	36
17.	Transient Compressor Measurements - Recovery from Stall . . . . .	37

## NOMENCLATURE

$A_i$	Duct cross-sectional area at inlet rake station, $\text{ft}^2$
$M_i$	Mach number at inlet rake station
$p_d$	Static pressure at discharge rake station, psf
$p_i$	Static pressure at inlet rake station, psf
$p_{t_d}$	Total pressure at discharge rake station, psf
$p_{t_i}$	Total pressure at inlet rake station, psf
$Q_i$	Inlet volume flow, cfs
$R$	Gas constant, $\text{ft}^2/\text{sec}^2 \text{ } ^\circ\text{R}$
$r$	Radius of third stage ducts, ft
$T_{t_d}$	Total temperature at discharge rake station, $^\circ\text{R}$
$T_{t_i}$	Total temperature at inlet rake station, $^\circ\text{R}$
$\beta$	Inlet guide vane angle, deg
$\gamma$	Ratio of specific heats (1.4 for air)
$\eta_t$	Compressor adiabatic efficiency based on total pressure ratio
$\lambda_s$	Static pressure ratio, $p_d/p_i$
$\lambda_t$	Total pressure ratio, $p_{t_d}/p_{t_i}$



## INTRODUCTION

The Plenum Evacuation System (PES) of the Arnold Center Propulsion Wind Tunnel Facility (PWT) is intended to perform various operational functions. These functions include plenum evacuation and exhausting to atmosphere of tunnel airflow during propulsion tests for both the Transonic and Supersonic Circuits, as well as support operations for the Rocket Test Facility.

The PES consists of ten identical compressors subdivided into two equal increments (see Fig. 1). The compressors of each increment may be used in parallel or in two stage series operation (four compressors in parallel discharging to the fifth). The aerodynamic performance characteristics of these compressors are reported in Ref. 1. In addition to the five identical compressors, each increment is equipped with a sixth compressor of smaller size which can only be operated in series with the aforementioned second stage compressor for three stage operation of each increment.

The results of the aerodynamic calibration of the third stage compressor of one increment are presented herein. The steady-state, pressure ratio-volume flow, compressor characteristics and associated efficiency values are presented. In addition, transient pressure measurements obtained during the definition of the compressor stall boundaries are included.

## APPARATUS

### FACILITY

The Transonic and Supersonic Circuits of the PWT (Fig. 1) are continuous-flow, closed-return, variable-density wind tunnels. The Mach number range of the Transonic Circuit is 0.5 to 1.6 and of the Supersonic Circuit, 1.5 to 4.0. The test sections of both circuits are 16 ft square and 40 ft long. The circuits are primarily intended for testing the aerodynamic performance of full-scale engine installations, large aircraft models, and large or full-scale missile configurations. A more extensive description of the facility is presented in Ref. 2.

---

Manuscript released by authors July 1961.

## PLENUM EVACUATION SYSTEM

The Plenum Evacuation System is composed of two identical groupings or increments of compressors, drive equipment, and associated ducts and valves. The second increment is shown in Fig. 2. It can perform the function of plenum suction with either one or two increments, as well as the separate functions of plenum suction with the first increment and tunnel scavenging with the second increment.

Each increment has five Allis Chalmers VA-1409 compressors, which are nine stage, uncooled, axial-flow machines, and one Allis Chalmers VA-1107 compressor, which is a seven stage, axial-flow machine. The arrangement of the ducts and valves of each increment permits the compressors to be operated in one, two, or three stage compressor configurations.

The VA-1409 compressors are each rated at 4620 cfs (measured at 100°F) at a design pressure ratio of 3.3, and the third stage VA-1107 compressors have a design point at 1250 cfs (100°F) at a pressure ratio of 2.0. The compressors operate at a constant speed of 3600 rpm. All compressors have inlet guide vanes which are remotely controllable through an angle range of  $\pm 15$  deg from design conditions. A photograph of the third stage compressor is presented in Fig. 3.

The compressors are driven in groups of two by a common drive system; this makes a total of three drive groups for each increment (note Figs. 1 and 4). Two groups consist of two VA-1409 compressors driven in tandem by a 28,500-hp synchronous motor and a 2500-hp wound-rotor motor, and one group of one VA-1409 and one VA-1107 is driven in tandem by a 14,000-hp synchronous motor and a 1500-hp wound-rotor motor. The third stage compressor (VA-1107) can be disconnected from its drive group when three stage operation is not required. The total drive power of each increment is 77,500 hp at 100 percent rated load; however, a continuous service factor of 15 percent provides an available power figure of 89,000 hp.

## INSTRUMENTATION

The steady-state total pressures in the inlet and discharge ducts were determined by using area-weighted, pressure measuring rakes, the locations of which are indicated in Fig. 5. The rake details (location of thermocouples and pressure orifices) are presented in Fig. 6. The inlet and discharge steady-state static pressures were determined by use of four equally spaced wall static pressure taps mounted on the duct circumference in the plane of each rake. Four wall-mounted thermocouples were installed in the plane of the rake in the discharge duct in addition to the rake-mounted thermocouples.

The steady-state pressures were measured by manometers using either dibutyl phthalate (specific gravity of 1.045 at 70°F) or tetrabromoethylene (specific gravity of 2.902 at 70°F), depending on the range of the pressures to be measured. The thermocouple readout system consisted of two Brown self-balancing recording potentiometers, one for each rake station.

Transient pressures at inlet and discharge locations (note Fig. 5) in the third stage compressor ducts were measured by 0 to 15 psia high-response pressure transducers and were then recorded on a multichannel visicorder.

### TEST PROCEDURE

The objective of the test program was to determine the aerodynamic performance of the third stage compressor of the first increment. The tests were conducted with the Plenum Evacuation System isolated from the Transonic and Supersonic Circuits.

The tests were initially attempted with the third stage compressor flow recycled through its unit bypass duct and Valve No. 55, as shown in Fig. 4. However, during this operation the compressor pressure ratio and volume flow measurements indicated that the compressor was not operating along its predicted characteristic. Evaluation of these results and of the flow capabilities of the unit bypass ducts resulted in the conclusion that the 16-in.-diam bypass was too small. Therefore, the bypass duct and valve were modified, as shown in Fig. 7, by removing the valve from its original position immediately downstream of a tee connection to a position more suitable for flow control, and by installing an additional one-ft-diam bypass duct and valve. Subsequent operation proved these modifications to be adequate to bypass the third stage compressor flow and to operate on its normal characteristic.

The compressor tests were conducted with the compressor flow recycled via its unit bypass or through the PES bypass. Variations of the compressor pressure ratio were obtained by manipulations of the pertinent bypass valve and/or either the compressor inlet Valve No. 51 or discharge Valve No. 53.

The majority of the data were obtained at compressor inlet pressures between 600 and 700 psfa and a nominal inlet temperature of 100°F. The compressor stall boundary was determined at inlet guide vane settings of +15, 0, and -15 deg.

Data were also obtained at an inlet temperature of 135°F to determine the effect of variation of inlet temperature on the compressor performance.

In addition to the steady-state measurements of compressor total and static pressure ratios, compressor efficiency, and inlet volume flow, transient pressure measurements were obtained at various locations in the third stage compressor ducts prior to, during, and subsequent to operating the compressor in stall.

### DATA REDUCTION PROCEDURE

The total pressure on the inlet and discharge sides of the compressor were determined from the area-weighted inlet and discharge rake readings, respectively. The inlet and discharge static pressure values were obtained at their respective survey stations by averaging the readings of the wall static pressure taps. The inlet and discharge total temperature values were determined by averaging all the thermocouple readings at their respective survey stations.

The following basic equations were used in calculating the compressor performance results presented in this report:

$$\text{Inlet Volume Flow} \quad Q_i = 49.0 A_i M_i \sqrt{\frac{T_{ti}}{1 + 0.2 M_i^2}} \quad (1)$$

$$\text{Total Pressure Ratio} \quad \lambda_t = \frac{p_{td} - p_{ti}}{p_{ti}} + 1 \quad (2)$$

$$\text{Static Pressure Ratio} \quad \lambda_s = \frac{p_d - p_i}{p_i} + 1 \quad (3)$$

$$\begin{array}{l} \text{Compressor Adiabatic} \\ \text{Efficiency Based on Total} \\ \text{Pressure Ratio} \end{array} \quad \eta_t = \frac{\lambda_t^{\frac{\gamma-1}{\gamma}} - 1}{\frac{T_{td}}{T_{ti}} - 1} \quad (4)$$

## RESULTS AND DISCUSSION

### STEADY-STATE COMPRESSOR CHARACTERISTICS

#### Measured Compressor Performance

The compressor total pressure ratio-volume flow characteristics measured at an inlet temperature of 100°F and inlet pressures between 600 and 700 psfa are presented in Fig. 8. With change of inlet guide vane angle from +15 to -15 deg the maximum total pressure ratio increased from 2.15 to 2.26. At the compressor design pressure ratio of 2.00 the maximum volume flow increased from 1425 to 1600 cfs with change of blade angle setting. The measured compressor adiabatic efficiency varied from 45 to 89 percent with variation of pressure ratio from 1.3 to 2.26.

Since the anti-surge and pressure ratio instrumentation used for monitoring the compressor during normal operation utilizes static pressure measurements at the compressor inlet and discharge, a comparison of the measured total and static pressure ratios is made in Fig. 9. Because of the velocity differences of the inlet and discharge airflows, the static pressure ratios were between 0.13 and 0.08 units lower than the comparative total pressure ratios.

#### Effect of Inlet Temperature on Performance

The third stage compressor was operated at the design (zero-deg) inlet guide vane setting at an inlet temperature of 135°F to determine the influence of inlet temperature on the compressor performance. The compressor flow was recycled through the compressor unit bypass in order to minimize duct radiation losses. Because of the compressor aftercooler exit air temperature limitation of 160°F and duct heat losses, the maximum compressor inlet temperature realized was 135°F. The throttling characteristic of the unit bypass limited the minimum pressure ratio of the compressor to 1.84.

Comparison of the compressor characteristic for zero-deg inlet guide vane angle setting measured at inlet temperatures of 135 and 100°F are presented in Fig. 10. Increasing the inlet temperature from 100 to 135°F decreased the maximum compressor pressure ratio capabilities from 2.22 to 2.17 and the inlet volume flow value at pressure ratio 2.0 from 1415 to 1350 cfs.



### Comparison of Measured and Predicted Compressor Performance

The measured and predicted compressor performance characteristics at an inlet temperature of 100°F for inlet guide vane angle settings of +15, 0, -15 deg are presented in Fig. 11. The predicted characteristics were furnished by the compressor contractor. The volume flow capabilities of the compressor exceeded the predicted values at all guide vane settings. At the design blade angle setting of zero deg and the design pressure ratio of 2.0, an inlet volume flow of 1415 cfs was realized as compared with the predicted value of 1250 cfs. The range of maximum pressure ratio for both the measured and predicted characteristics were nearly identical.

The measured adiabatic efficiency of the compressor at the design point ( $\lambda = 2.00$ ) was 87 percent as compared with the predicted value of 82 percent.

### Compressor Maximum Inlet Pressure Capabilities

The maximum inlet pressure range of the compressor for maximum ( $\beta = -15$  deg), design ( $\beta = 0$  deg), and minimum ( $\beta = +15$  deg) flow conditions is presented in Fig. 12. The maximum pressures are limited by a power input to the compressor of 3800 hp, which is the rating of the coupling connecting the second and third stage compressors.

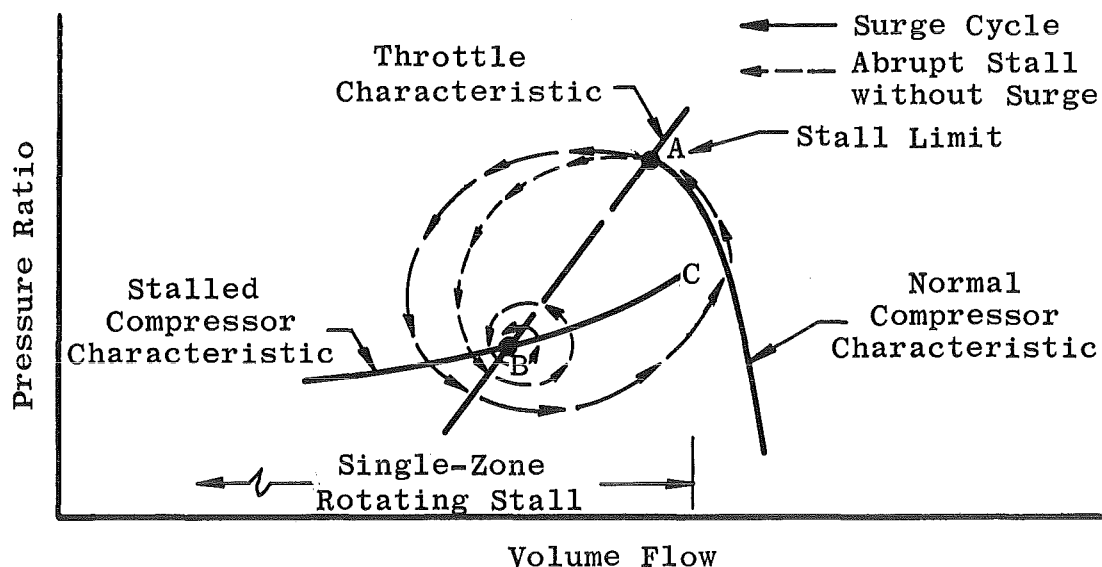
### COMPRESSOR DOUBLE-VALUED PERFORMANCE CHARACTERISTIC

Measurements obtained during the initial operation of the third stage compressor with the flow being recycled through the compressor unit bypass indicated an unusual operational circumstance. The pressure ratio-volume flow results (Fig. 13) indicated that the compressor did not operate along its expected performance characteristic, but instead operated in an apparently stable manner at an inlet volume flow-pressure ratio value (Point B) which was considerably less than expected. The compressor efficiency during this operation was approximately 30 percent, which is about one-half the normal value at this pressure ratio. Closing the bypass valve a small amount caused a slight reduction of compressor pressure ratio and a decrease of inlet volume flow, as shown by curve B-D of Fig. 13. The compressor was evidently operating along a stalled portion of the performance characteristic.

As previously noted by other investigators (Refs. 3 and 4), multistage compressors may have double-valued performance characteristics. In addition to the normal characteristic, a characteristic representative of the presence of rotating stall may exist. Rotating stall consists of one or more zones of stalled flow that rotate about the compressor axis and may be categorized as either progressive or abrupt stall. Progressive stall is characterized by a gradual but continuous decrease in performance after stall inception, resulting from the formation of a rotating stall pattern consisting of more than one stall zone. Abrupt stall, characterized by an abrupt or discontinuous decrease in compressor performance at instigation of stall, is associated with a single zone stall pattern. Normally, during performance tests of a multistage compressor, these discontinuities are not observed, since compressor surge is encountered. However, compressor stall and surge represent the same limit of compressor operation.

The operation along the stalled portion of the compressor characteristic, such as shown in Fig. 13, is not normally realized since flow oscillations present during stall exceed the flow value required for recovery from stall, and a continuous cycle of stall and recovery will occur. This cyclic stalling and unstalling of the compressor provide the mechanism for surge.

Whether a compressor will experience surge when operated beyond the stall limit is a function of the compressor characteristic, throttling valve characteristic, and volumes of the inlet and discharge ducts. The accompanying sketch shows the approximate paths involved during compressor stall and surge.



The operation of the compressor beyond the stall point A at design rotational speed will instigate breakdown of normal flow conditions in the downstream compressor stages and the formation of a single zone of rotating stall. The stall zone generally covers approximately one-third of the compressor annulus and has an absolute rotational speed of 30 to 40 percent of the rotor speed. This type of stall is associated with a discontinuous performance characteristic that is coincident with an abrupt drop of compressor pressure ratio. Operation beyond the stall limit (Point A) will cause surge conditions if the compressor and the system characteristics are such that the amplitude of the flow instabilities (transients) are sufficient to match the flow value (Point C) required to permit recovery from stall. The flow must be increased to a value (Point C) somewhat greater than the stall inception value (Point A) in order to relieve the stalled flow condition.

Flow oscillations (surge) may exist during stall if the associated ducts at the compressor inlet and discharge have relatively large volumes. The large volumes do not allow a rapid adjustment of pressure subsequent to stall and consequently do not damp out flow oscillations quickly. Small duct volumes, which adjust rapidly to pressure changes, tend to damp out flow transients and therefore reduce the probability of surge conditions.

The discovery that the third stage compressor can operate in the stalled mode on its unit bypass necessitated immediate corrective action. An estimate of the bypass throttling characteristic as shown in Fig. 13 illustrates how the stall limit was exceeded. In order to match the bypass throttling characteristic, an additional one-ft-diam bypass duct and valve were installed, and the bypass ducts were modified as mentioned under Test Procedure. This provided a matching point at a total pressure ratio of about 2.0, which is less than the compressor stall limit when both of the unit bypass valves are fully open.

#### TRANSIENT COMPRESSOR MEASUREMENTS

Transient pressure measurements were obtained during the definition of the stall boundary of the compressor. The transient pressure measurement stations (wall static pressure orifices) were located immediately upstream and downstream of the compressor, downstream of the compressor aftercooler, and in the large PES discharge duct (note Fig. 4).

The results of the transient pressure measurements are presented in Figs. 14 through 17. All data were obtained with the compressor operating via its unit bypass ducts (both the original duct and the supplemental one-ft-diam duct) with the compressor inlet Valve No. 51 closed and the compressor discharge Valve No. 53 open. The bypass throttling characteristic was varied by controlling the one-ft-diam bypass valve. It was necessary to operate with the compressor ducts vented to the PES large discharge duct via Valve No. 53 so that the compressor discharge pressure level during steady-state operation could be kept constant.

The data of Fig. 14 were obtained when the stall limit (Point A) was exceeded and the compressor settled out in a steady-state "stalled" condition (Point B) at a reduced volume flow and pressure ratio. The various measured pressures experienced fluctuations immediately after stall inception, but since the flow oscillations were not of sufficient magnitude to exceed the volume flow required to recover from stall (Point C of the accompanying sketch), the compressor settled out and operated at the intersection of the bypass characteristic and the stalled branch of the compressor characteristic (Point B).

As shown in Fig. 14, the steady-state value of approximately 2.15 for the static pressure ratio decreased to about 1.5, and the inlet pressure increased from approximately 320 to 480 psfa with the discharge pressure unchanged. The transition to the new steady-state pressure occurred in damped oscillation, which ceased after approximately 1.5 sec. This behavior can be expected because the duct-valve compressor system can be considered as a Helmholtz resonator system connected to a much larger volume through the resistance of the discharge Valve No. 53. Any sudden changes in steady-state values in such a system are accompanied by damped oscillations at about the natural frequency of the resonators. The PES discharge header pressure remains practically constant because of its large volume. The data of Fig. 14 indicate that the fundamental frequency of the transients is about 2.5 cps. The superimposed higher frequency at the compressor discharge might be caused by separation wakes in the stalled regions but subsequently filters out in the discharge ducts and cooler.

Of particular interest are the rates of change of the inlet and discharge pressures immediately after compressor stall inception. These rates of change are a function of the magnitude of the initial disturbance. The dashed lines on the pressure-time plot of Figs. 14, 15, and 16 at the stall point A are the rates of change of these two pressures

for the condition assuming the compressor volume flow suddenly going to zero, which is the maximum possible disturbance. A comparison of these calculated slopes with the measured pressure-time values indicates that at stall the compressor flow apparently broke down completely for a short time period.

During compressor operation on the stall characteristic, the oscillograph records showed a variation of discharge pressure at a frequency of about 24 cycles per second, which corresponds to 40 percent of the rotor design rpm of 3600. This variation of discharge pressure could be attributed to a zone of stalled flow rotating around the compressor at 40 percent of the rotor speed. These variations of pressure have not been transferred from the oscillograph recordings to the data of Figs. 14, 15, and 16.

The data of Fig. 15 were obtained when the stall limit (Point A) was exceeded and the compressor experienced a stall and stall recovery cycle (surge) prior to settling out at the stalled operating Point B. As represented schematically on the pressure ratio-volume flow sketch and the perturbations of the various transient pressures, the flow oscillations that occurred immediately after stall inception were of sufficient magnitude to allow the compressor to recover from stall. The compressor then followed up the normal characteristic to Point A where stall once again occurred. However, the flow oscillations that occurred subsequent to the second stall did not permit stall recovery, and the compressor converged on the operating point at the intersection of the stall characteristic and the bypass characteristic.

The third type of stall phenomena noted during the compressor stall boundary investigation is shown in Fig. 16. The compressor experienced continuous cycles of stall and stall recovery when the bypass characteristic exceeded the compressor stall limit. The compressor continued to surge until the bypass valve was opened and the bypass throttling characteristic intersected the normal compressor characteristic.

The various types of stall phenomena noted in Figs. 14, 15, and 16 may be attributed to a variation of only one of the three factors pertinent to whether stall or surge occurs. Of the three factors, bypass throttling characteristic, compressor characteristic, and the inlet and discharge duct volumes, only the bypass valve position (and therefore only the bypass characteristic) was varied when obtaining the data presented. A small closure of the bypass valve, so that the bypass characteristic is shifted only slightly beyond the

stall limit (Point A of Fig. 13), requires a minimum of flow oscillation during stall to match the flow required for stall recovery (Point C) and thus allows surge to occur, as shown in Fig. 16. A larger closure of the bypass valve, so that the bypass characteristic is shifted significantly past the stall limit, would require a larger oscillation of flow for stall recovery and the existence of subsequent surge conditions; this is representative of the data shown in Figs. 14 and 15.

Subsequent to the compressor operation along the stalled branch of the compressor characteristic, as shown in Figs. 14 and 15, the one-ft-diam bypass valve was reopened. The transient pressure variations from stalled to unstalled operation are shown in Fig. 17. The transition from stalled to unstalled condition was very different from that in going into stall. No instability or fluctuation of pressures occurred; instead, the inlet pressure decreased smoothly to a lower value, and the pressure ratio increased gradually to the normal operating pressure ratio of about 2.0. This might be explained by the assumption that the process of unstalling is smooth, whereas the stall process consists of sudden flow breakdown.

#### CONCLUDING REMARKS

An investigation of the aerodynamic performance of the third stage compressor of the Plenum Evacuation System at maximum ( $\beta = -15$  deg), design ( $\beta = 0$  deg), and minimum ( $\beta = +15$  deg) flow settings of the compressor inlet guide vanes produced the following results:

1. The measured compressor performance at the design inlet temperature of 100°F realized a maximum pressure ratio boundary of 2.15 to 2.26 with variation of inlet guide vane angle setting from +15 to -15 deg. The inlet volume flow capacity varied from 1285 to 1485 cfs at the compressor design pressure ratio of 2.00 with change of blade angle setting. The measured compressor adiabatic efficiency at the design condition was 87 percent. The measured performance exceeded or matched the predicted performance values in all aspects.
2. The compressor experienced a decrease of the compressor stall boundary from 2.22 to 2.17, and the maximum inlet volume flow decreased from 1545 to 1495 cfs with an increase of inlet temperature from 100 to 135°F during operation at the design inlet guide vane angle setting.

3. The compressor unit bypass duct and valve, as furnished by the contractor, proved to be inadequate to bypass the full flow of the compressor. A supplementary one-ft-diam bypass duct and valve were required in order to operate the compressor within its performance capabilities during the calibration program. The original and the temporary one-ft-diam bypass ducts will be replaced by a single 2.5-ft-diam bypass duct and valve.
4. The compressor exhibited a unique operational trait during definition of the compressor stall boundary. Depending upon the restriction of the bypass system, as established by controlling the bypass valves, the compressor experienced either stall or surge conditions. The unusual aspect discerned during operation was that the compressor, after experiencing the inception of stall, converged on an operating point defined by the intersection of the bypass characteristic and the stalled branch of the compressor characteristic and then operated in an apparently stable manner at this point. Although no significant net flow oscillations were present during the stalled operation, continued operation at these conditions is not justified because of the presence of rotating stall within the compressor which might cause blade failure by resonance. Continuous operation along the stalled characteristic is also not warranted because of the low compressor efficiency realized and attendant excessive drive power required.

#### REFERENCES

1. Estabrooks, B. B. "Aerodynamic Performance of the AEDC-PWT Plenum Evacuation Compressors." AEDC-TN-58-52, August 1958.
2. Test Facilities Handbook, (3rd Edition). "Propulsion Wind Tunnel Facility, Vol. 3." Arnold Engineering Development Center, January 1961.
3. Huppert, M. C. and Benser, W. A. "Some Stall and Surge Phenomena in Axial-Flow Compressors." Journal of the Aeronautical Sciences, Vol. 20, No. 12, December 1953, pp. 835-845.
4. Compressor and Turbine Research Div. "Aerodynamic Design of Axial-Flow Compressors, Vol. III." NACA RM E56B03b, August 1956.

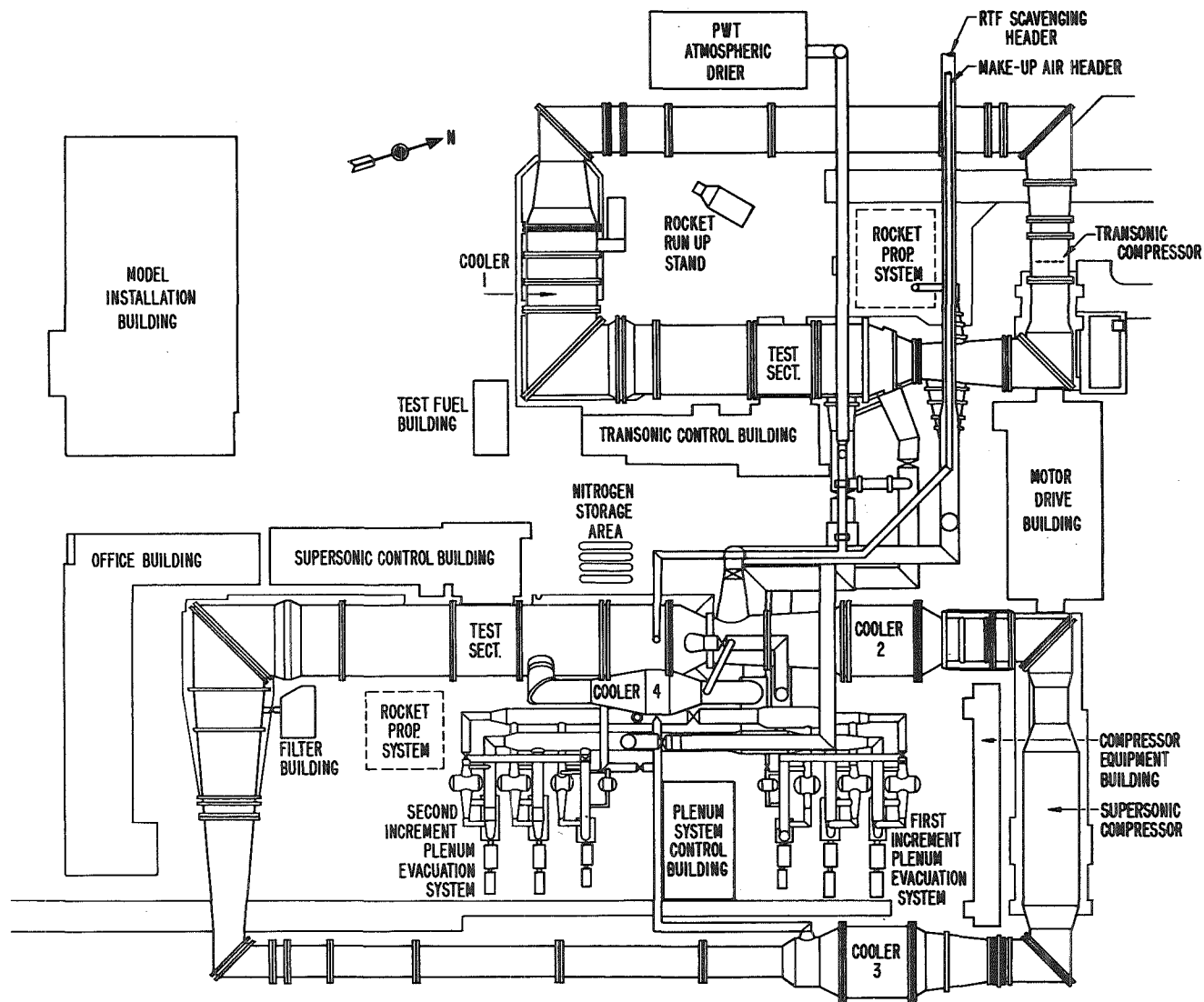


Fig. 1 The PWT Facility Layout



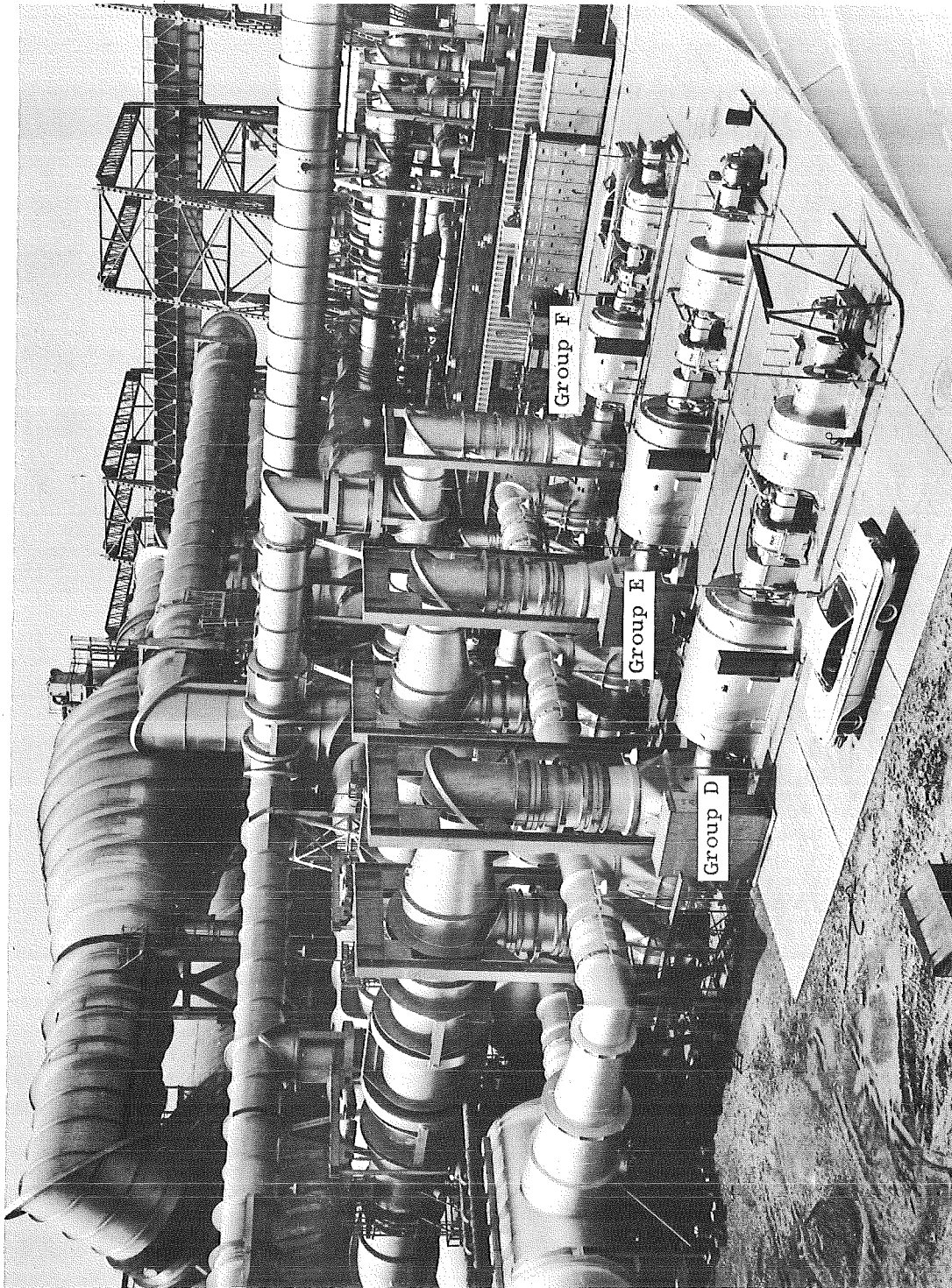


Fig. 2 View of the Plenum Evacuation System (Second Increment)

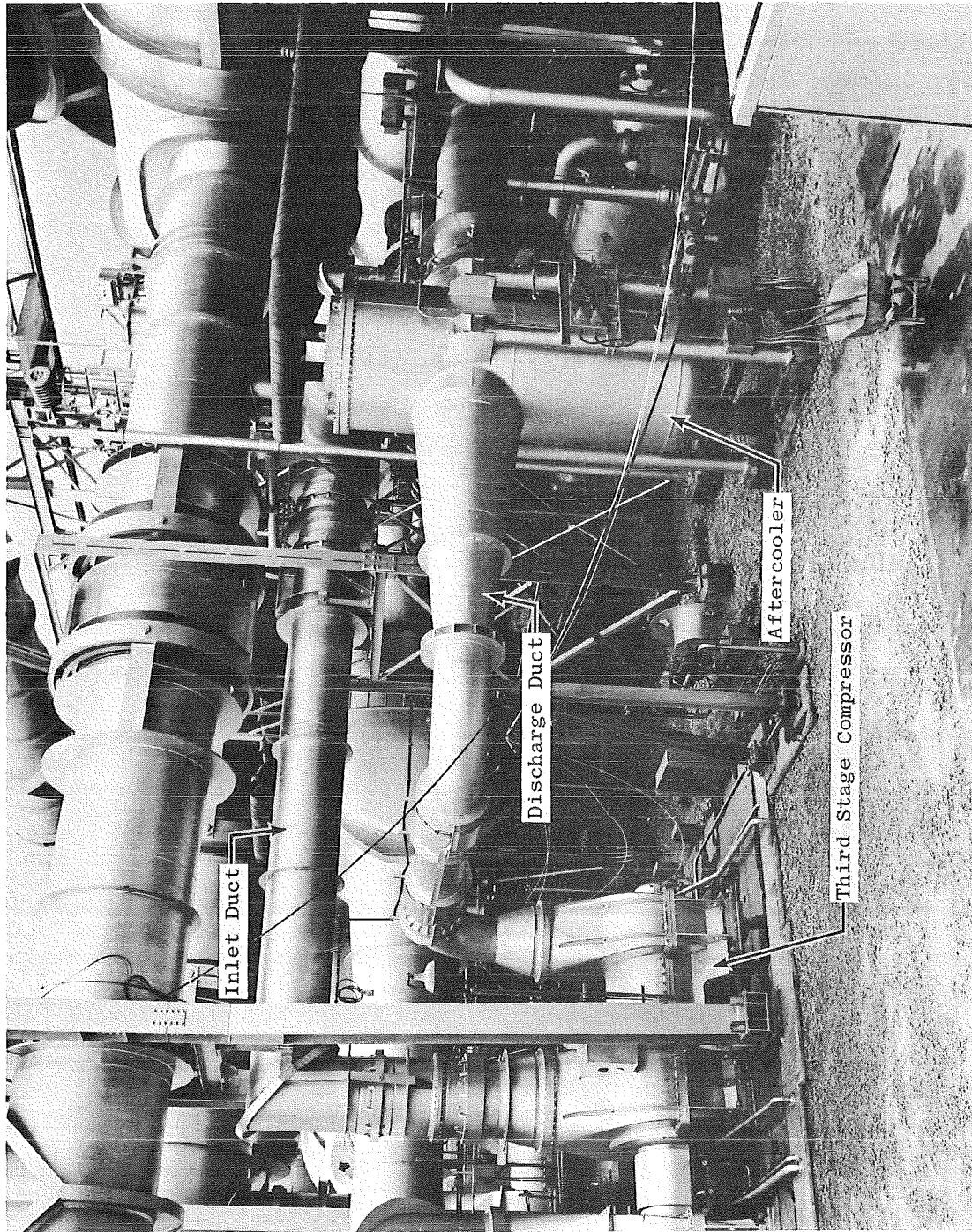


Fig. 3 Third Stage Compressor and Associated Ducts

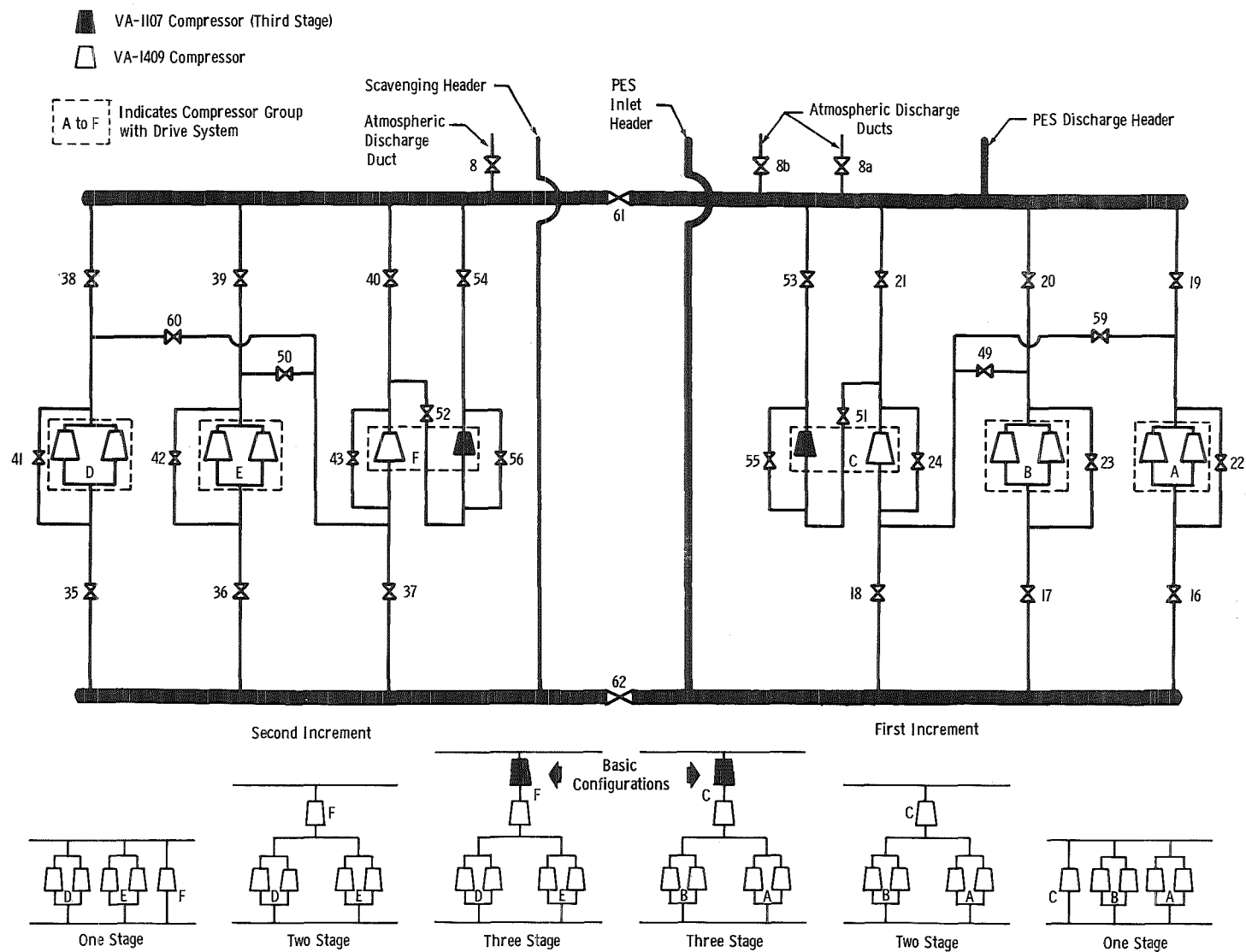


Fig. 4 Schematic of Plenum Evacuation System

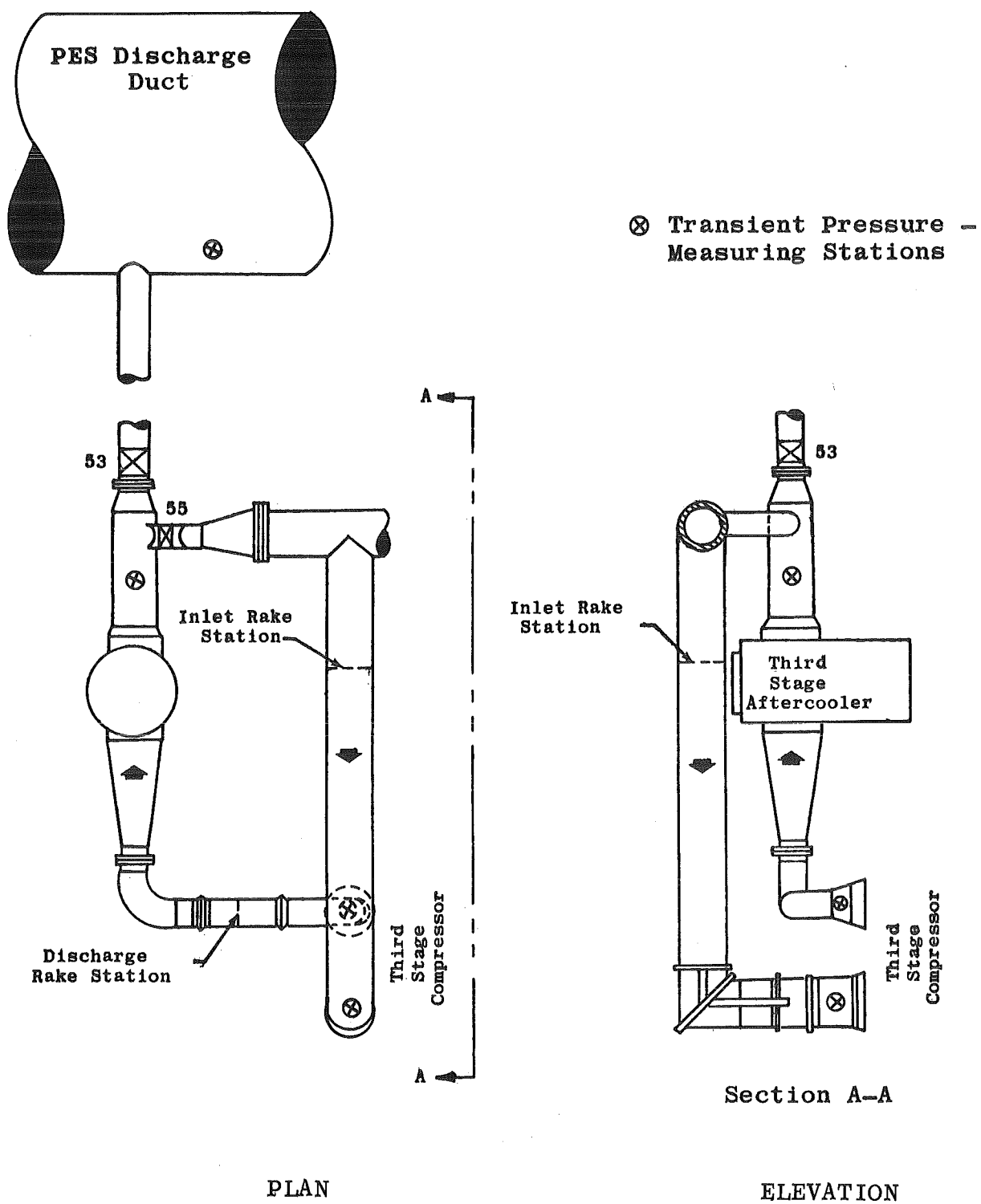


Fig. 5 Layout of Third Stage Compressor Ducts and Aerodynamic Instrumentation Locations

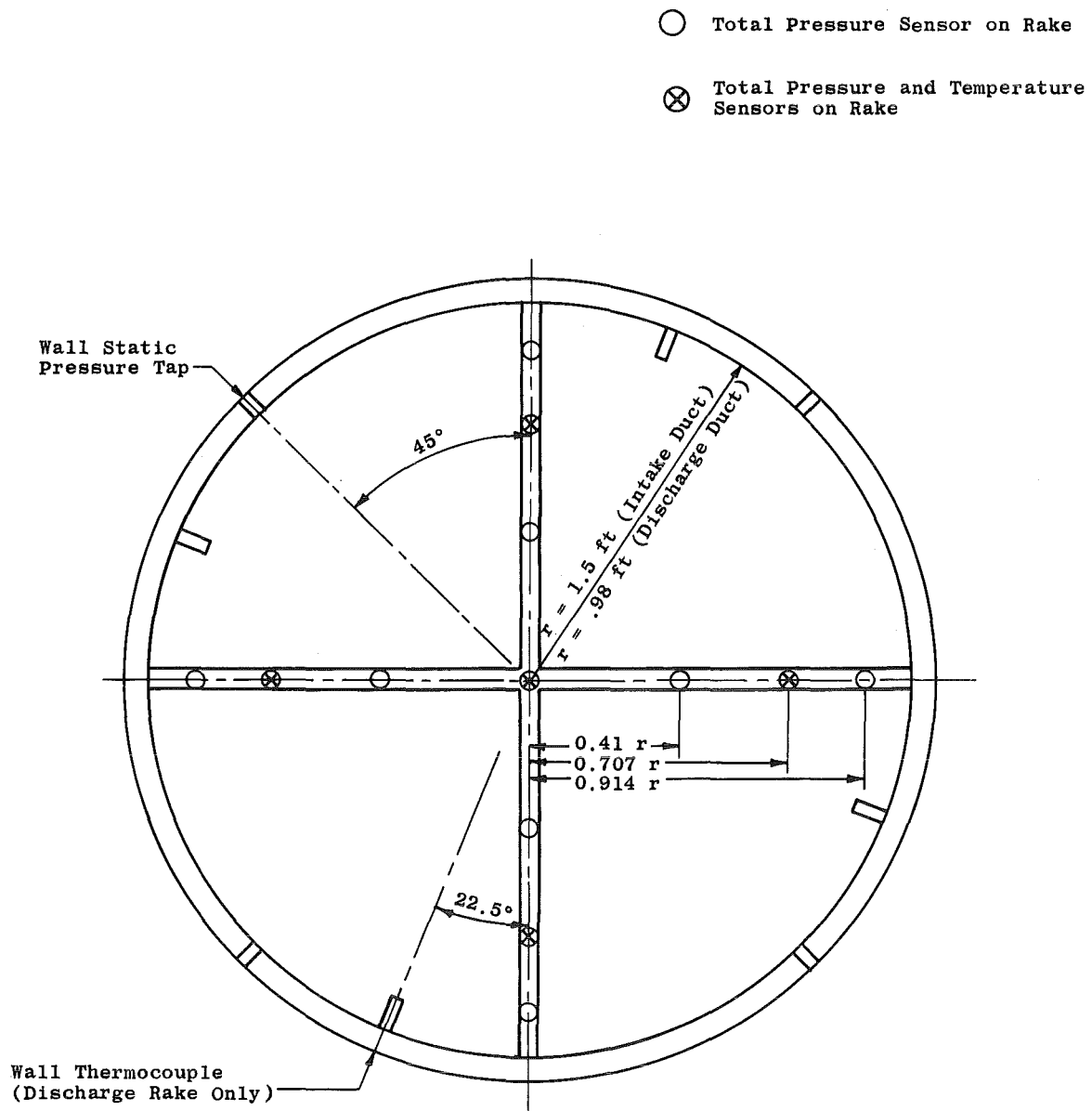
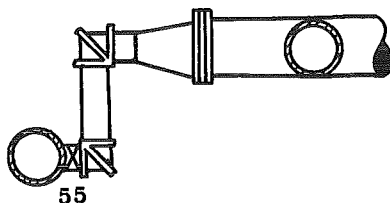
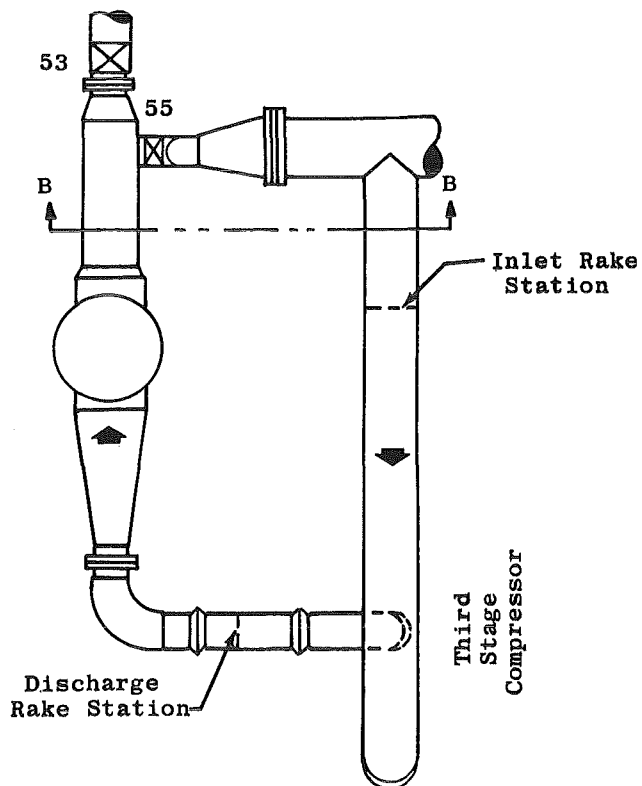
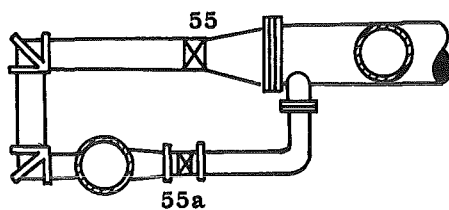


Fig. 6 Dimensions and Details of Rake Installations



Section B-B Before Modification



Section B-B After Modification

Fig. 7 Layout of Third Stage Compressor Bypass Ducts Arrangement

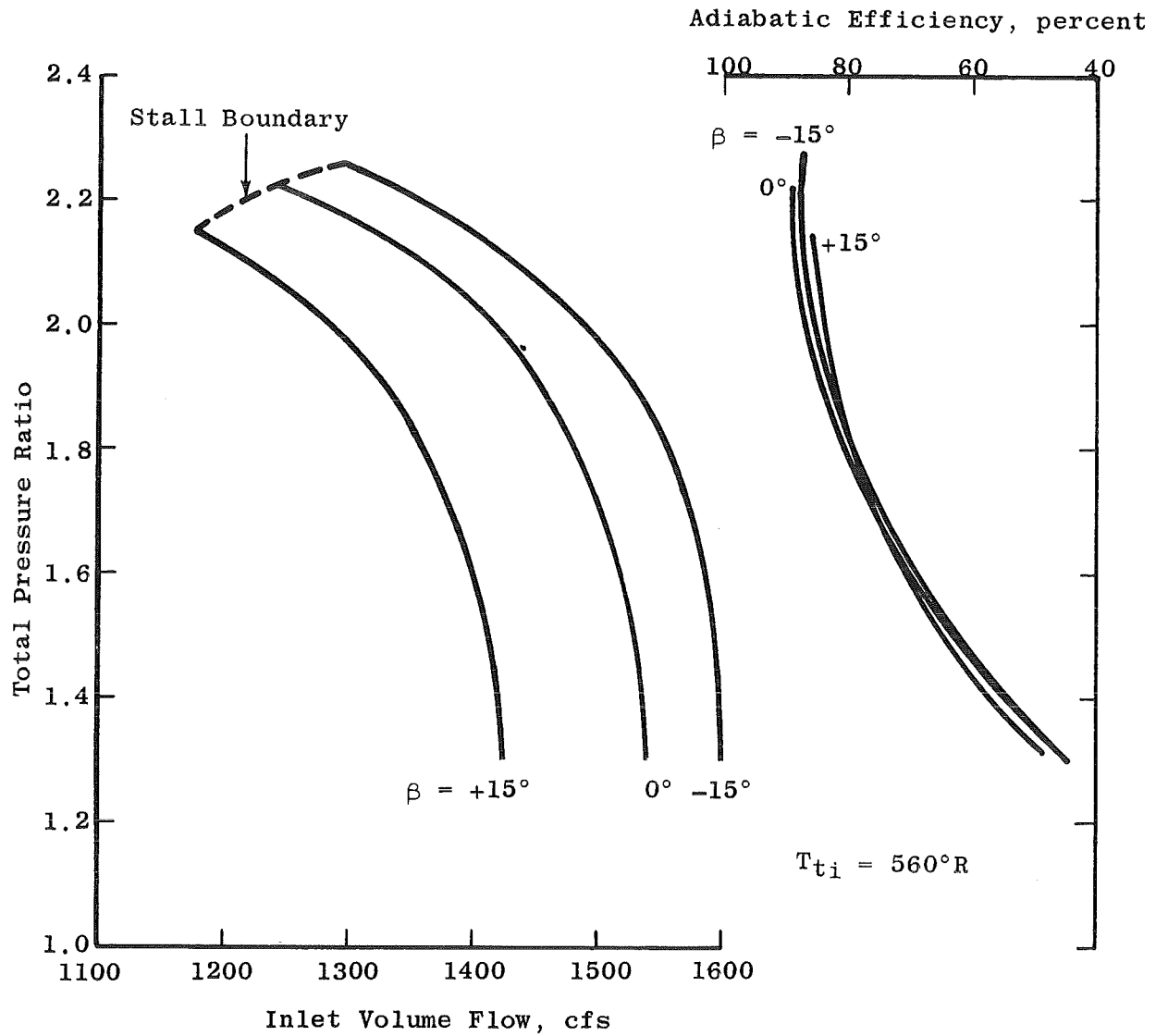


Fig. 8 Measured Compressor Performance at 100°F Inlet Temperature

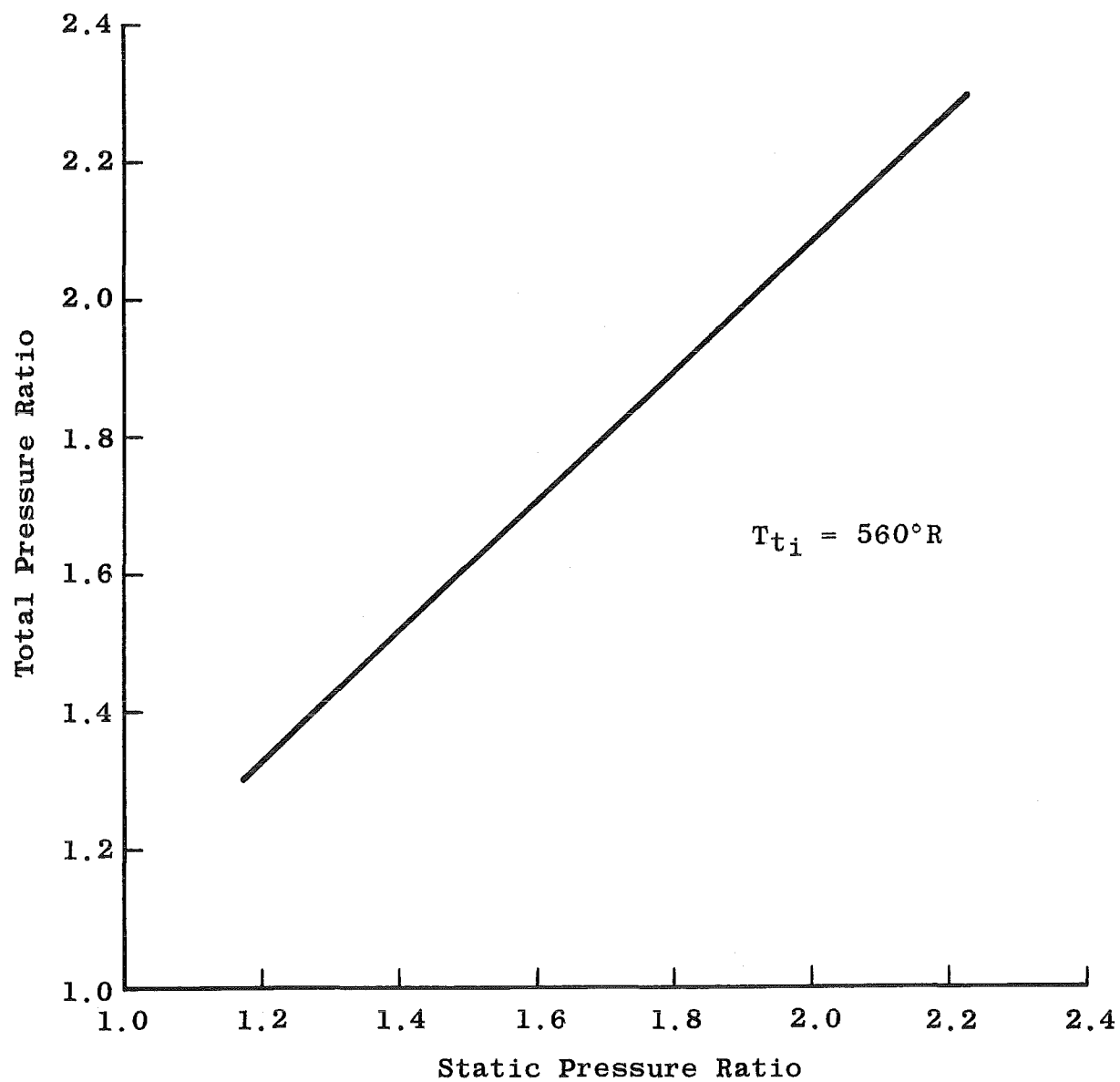


Fig. 9 Comparison of Total and Static Compressor Pressure Ratios



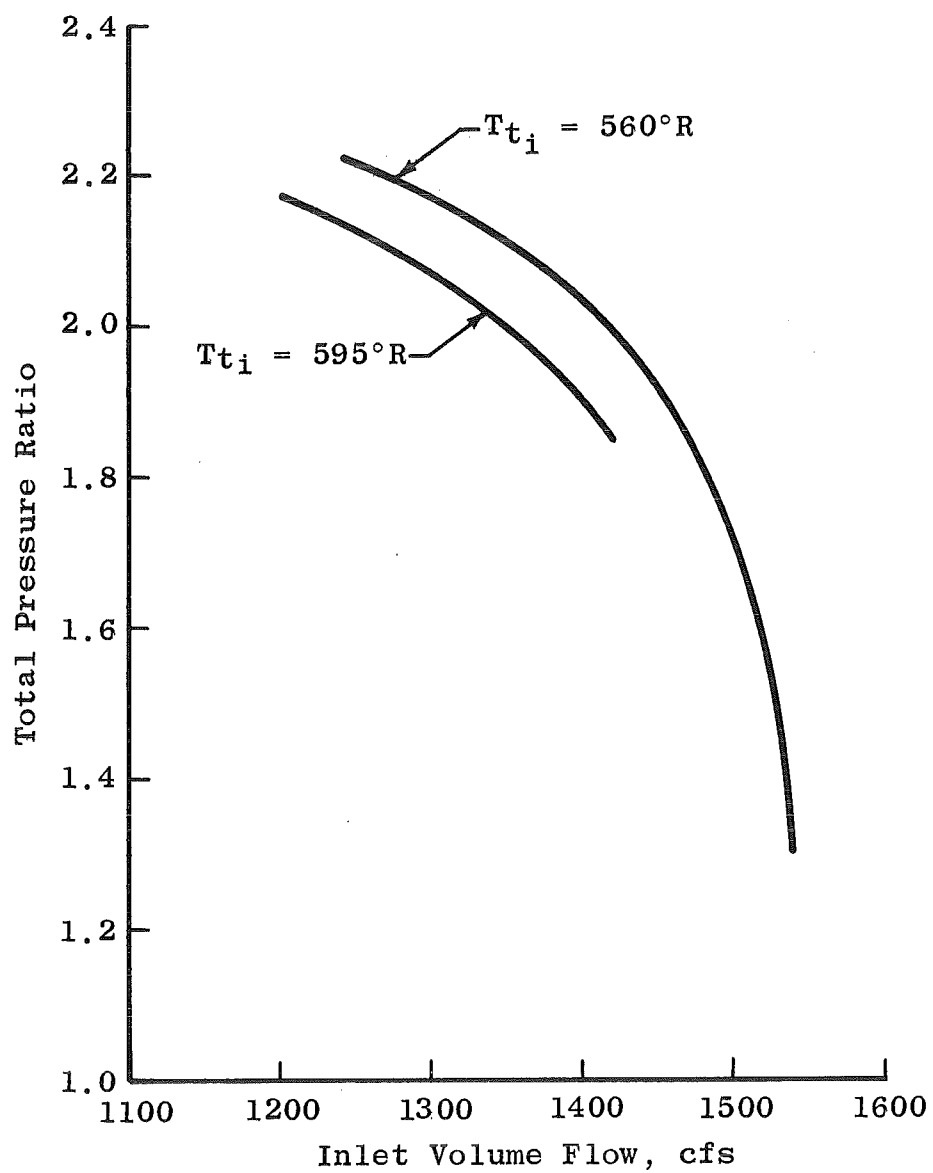


Fig. 10 Measured Compressor Performance at 135°F Inlet Temperature

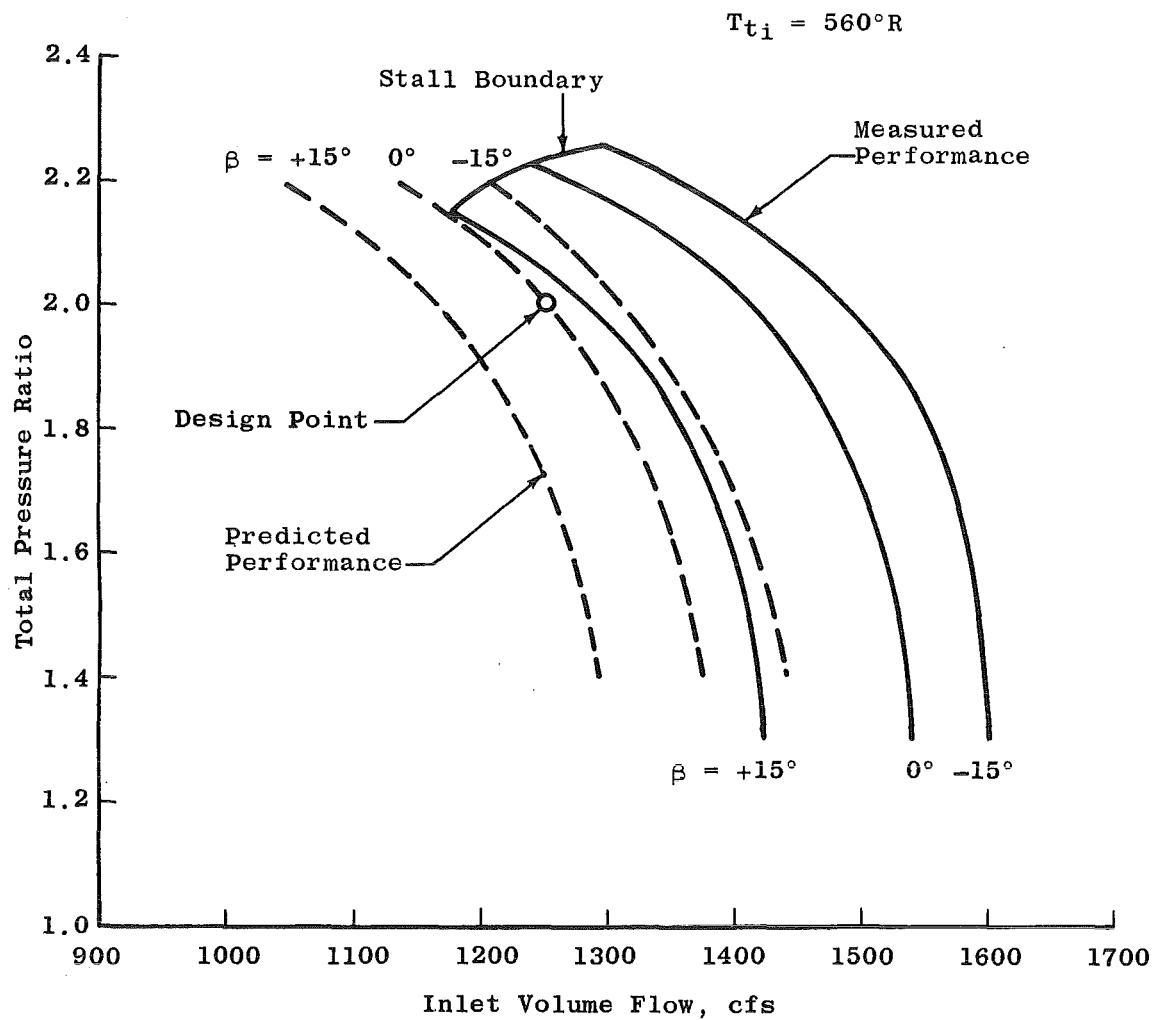


Fig. 11 Comparison of Measured and Predicted Compressor Performance

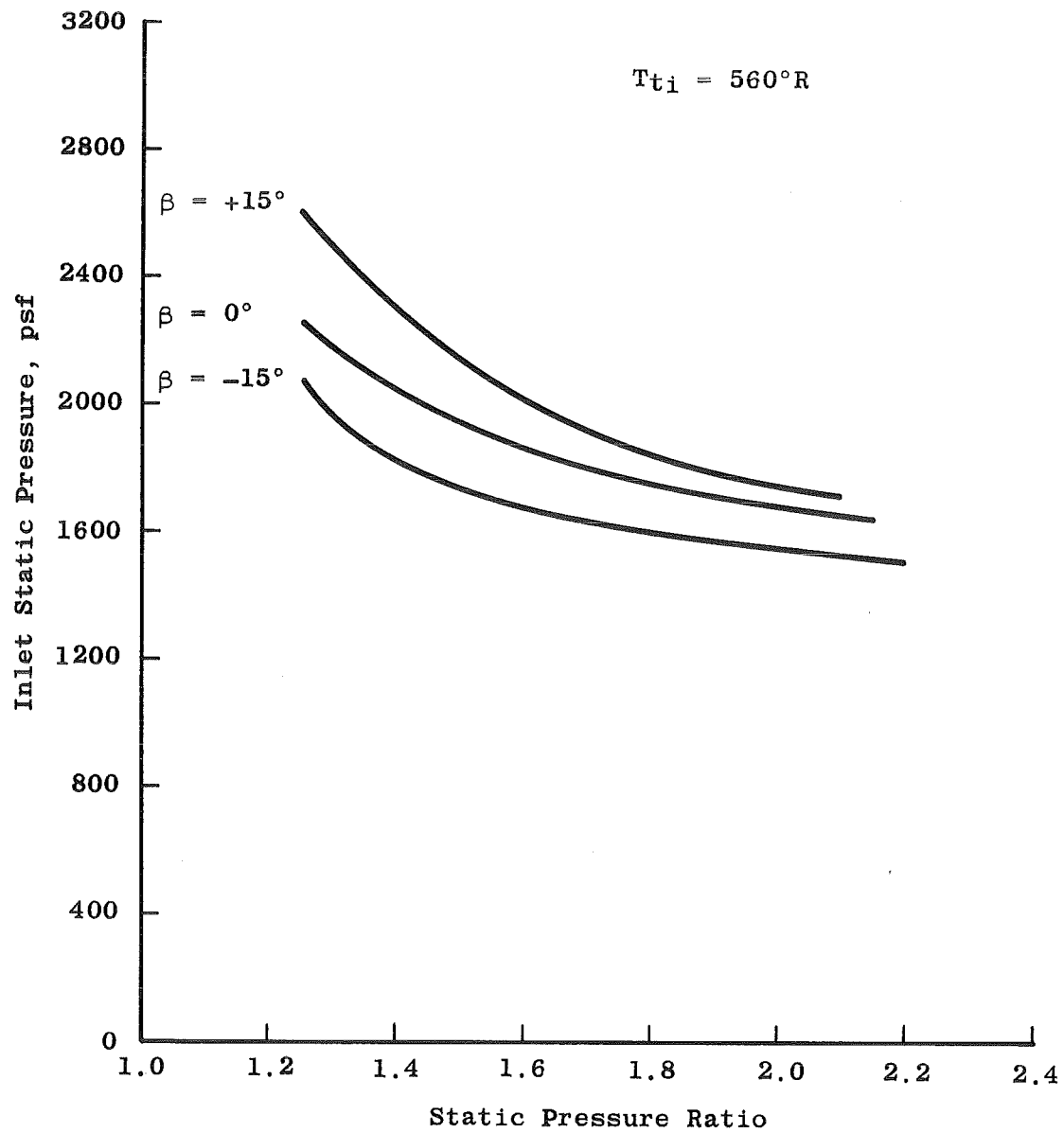


Fig. 12 Maximum Inlet Pressure versus Static Pressure Ratio of the Third Stage as Limited by Coupling Rating of 3800 hp

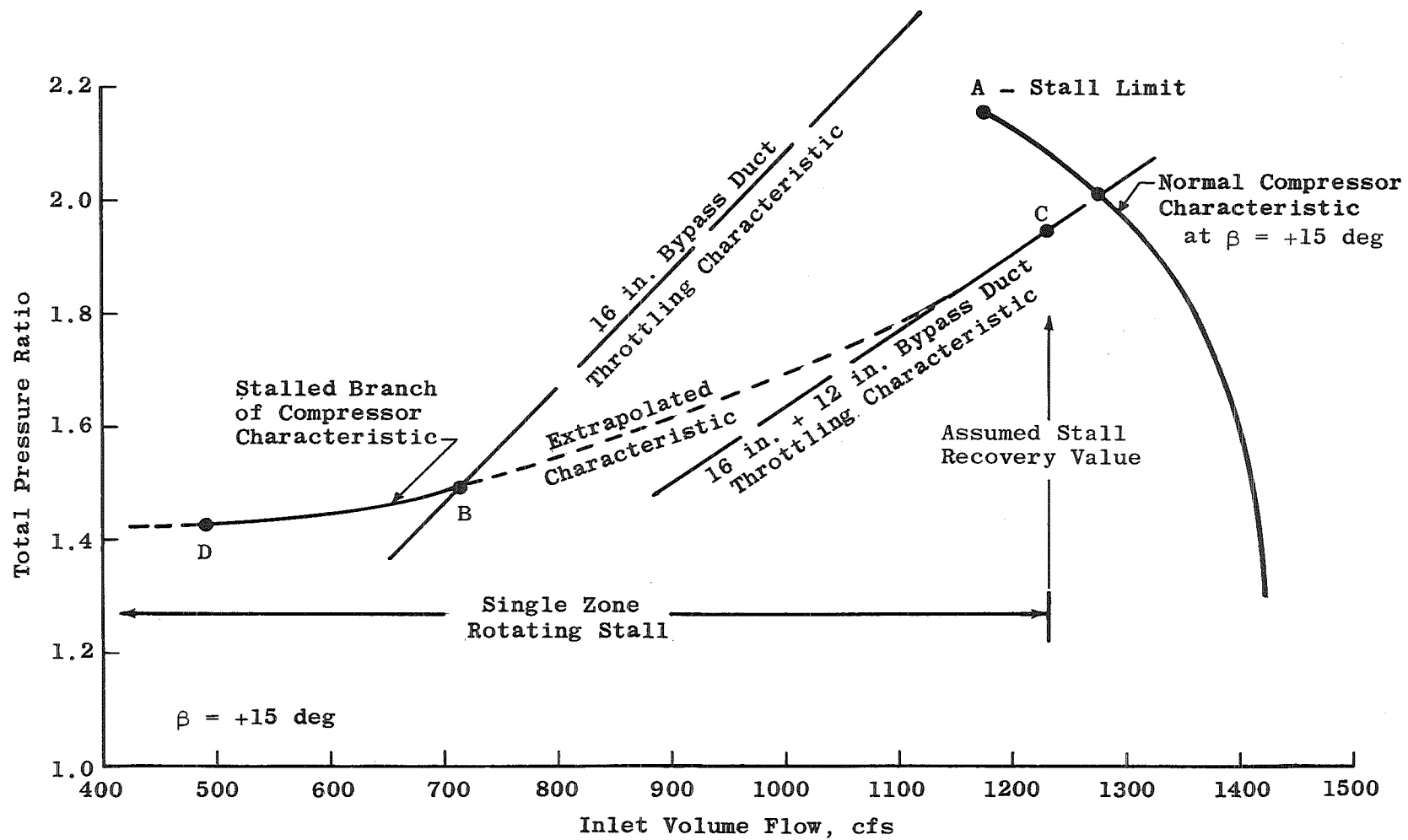


Fig. 13 Compressor Double-Valued Characteristics

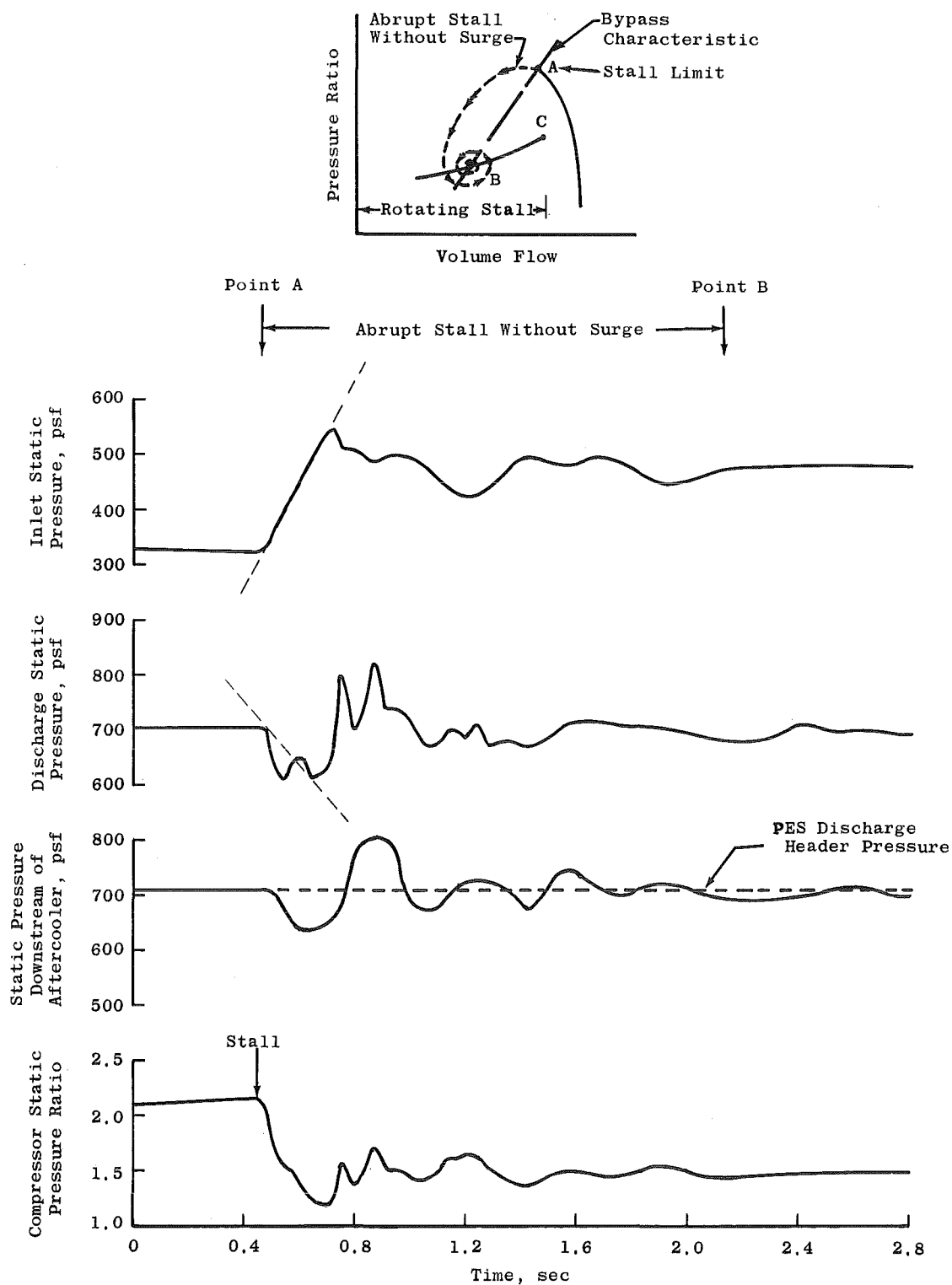


Fig. 14 Transient Compressor Measurements - Compressor Stall

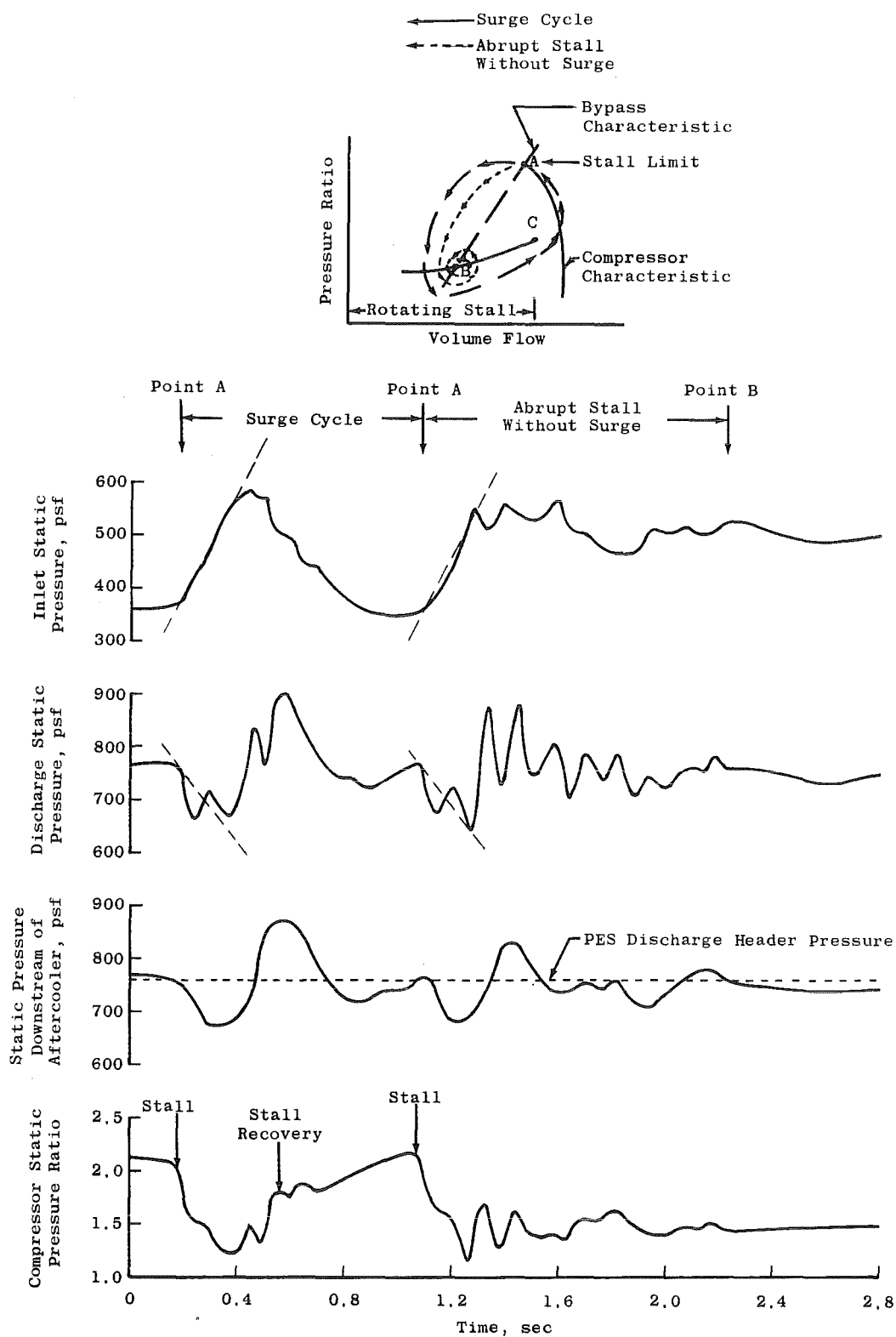


Fig. 15 Transient Compressor Measurements - Compressor Surge and Stall

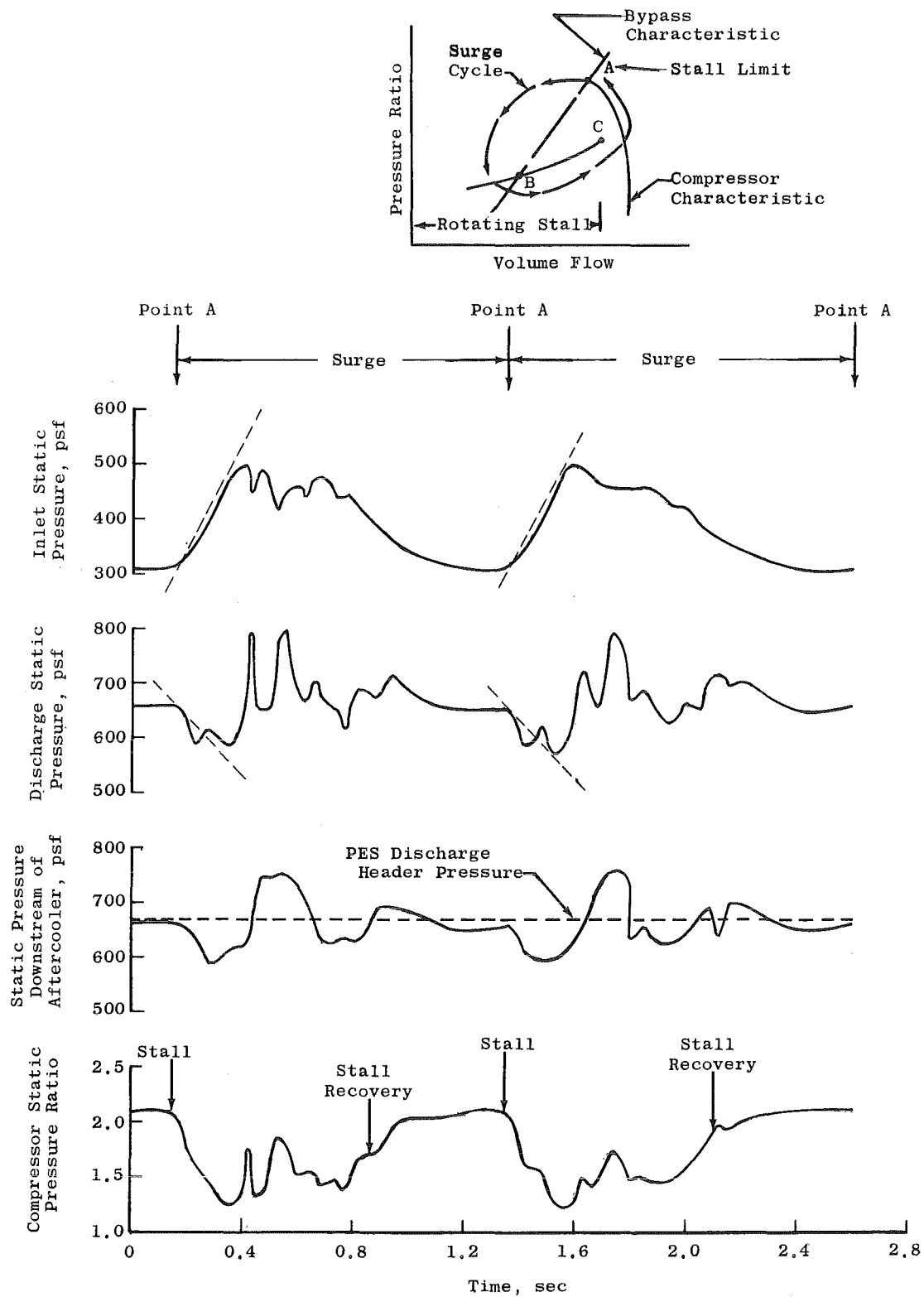


Fig. 16 Transient Compressor Measurements - Compressor Surge

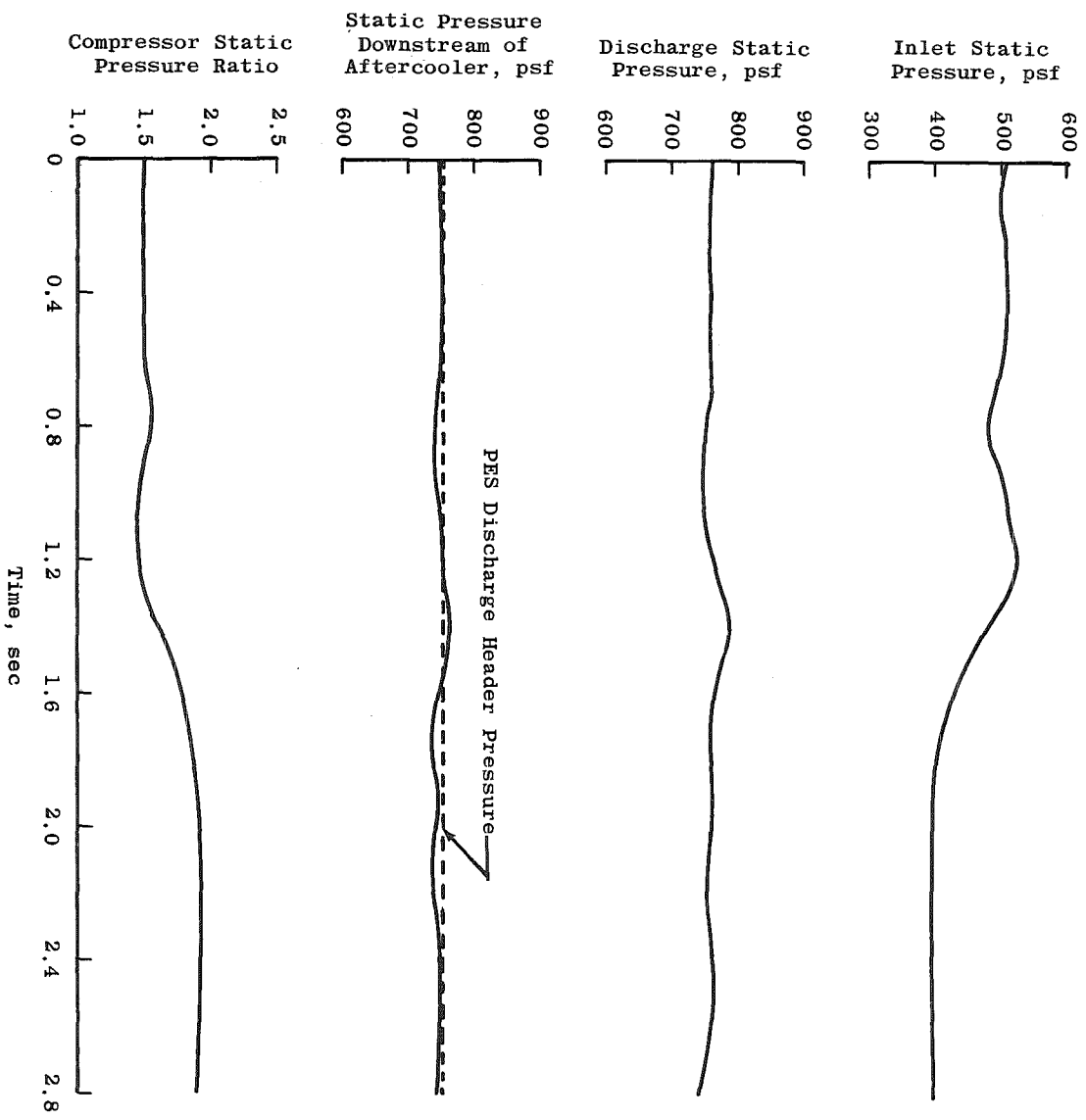


Fig. 17 Transient Compressor Measurements - Recovery from Stall